Biological Trace Element Research
https://doi.org/10.1007/s12011-024-04360-9

RESEARCH

Tannic Acid Suppresses Ferroptosis Induced by Iron Salophene Complex in Kidney Cells and Prevents Iron Overload-Induced Liver and Kidney Dysfunction in Rats

Indra Putra Taufani[1,2] · Sri Tasminatun[3] · Sabtanti Harimurti[3] · Liang-Yo Yang[4,5] · Chih-Yang Huang[6,7,8,9,10] · Jiro Hasegawa Situmorang[11]

Received: 31 May 2024 / Accepted: 26 August 2024

Abstract
Iron toxicity intricately links with ferroptosis, a unique form of cell death, and is significantly influenced by lipid peroxidation. Despite its critical role in various diseases and drug development, the association between iron toxicity and ferroptosis remains relatively unexplored. Accidental iron ingestion has emerged as a growing concern, resulting in a spectrum of symptoms ranging from gastrointestinal discomfort to severe outcomes, including mortality. This research introduces tannic acid (TA), which contains numerous phenol groups, as a powerful antiferroptotic agent. In male Wistar rats, even a modest dose of TA (7.5 mg/kg) significantly curtailed thiobarbituric acid reactive substances (TBARS), a well-established indicator of lipid peroxidation, and mitigated iron accumulation induced by ferrous sulfate ($FeSO_4$) in the liver and kidney. The evidence supporting TA's protective function against iron-triggered liver and kidney dysfunction was substantiated by assessing specifically the levels of blood urea nitrogen (BUN) and alanine aminotransferase (ALT). In cell models using ferroptosis inducers such as iron-salophene (FeSP) and RAS-selective lethal 3 (RSL3), tannic acid (TA) exhibited superior protective capabilities compared to the traditional iron chelator, deferoxamine (DFO). Nrf2 and HO-1, regulators of antioxidant defense genes, are implicated in controlling ferroptosis. The expression of Nrf2 and HO-1 increased with TA treatment in the presence of FeSP, indicating their role in reducing lipid ROS levels. Additionally, TA significantly reduced the heightened levels of COX2, a marker associated with ferroptosis. In summary, the remarkable antiferroptosis activity of TA is likely due to its combined iron-chelating and antioxidant properties. With its safety profile for oral consumption, TA may offer benefits in cases of accidental iron ingestion and conditions like hemochromatosis.

Keywords Ferroptosis · Hemochromatosis · HO-1 · Iron Toxicity · Nrf2 · Tannic Acid

Introduction

Ferroptosis, a term coined to describe iron-dependent cell death, was proposed just over a decade ago [1]. Although it was initially observed three decades ago and the term 'oxytosis' was used two decades ago, 'ferroptosis' has become the predominant term in current literature [2]. The defining characteristic of ferroptosis is an increased level of lipid peroxidation in the membrane phospholipids, which can lead to membrane damage. Iron, being the primary catalyst for triggering lipid peroxidation, remains a critical factor in the occurrence of ferroptosis through Fenton reaction [3]. Over the years, it has become evident that ferroptosis is involved in various diseases affecting vital organs such as the kidneys, liver, brain, heart, and lungs [4, 5]. A recent toxicological study revealed that the highest accumulation of the lipid peroxidation product malondialdehyde (MDA) occurs 12 h after a large dose of intraperitoneal injection of iron. This accumulation was most prominently observed in the kidney (3.1-fold increase), liver (3.2-fold increase), and ileum (1.5-fold increase) [6]. Several key proteins involved in antioxidant defense, such as gluthathione peroxidase 4 (GPX4) [7], nuclear factor erythroid 2–related factor 2 (Nrf2) [8], and heme oxygenase-1 (HO-1) [9], have been found to play a crucial role in protecting against ferroptosis. Furthermore, researchers widely employ GPX4 inhibition as a method to model ferroptosis in both in vitro and in vivo studies [10].

Tannic acid (TA) is a compound belonging to the group of tannins, which are astringent polyphenols consisting of

Extended author information available on the last page of the article

multiple gallic acid units at the periphery and a glucose at its core. This compound is widely known for its biomedical applications, including its use as a crosslinking agent in hydrogels and polymers [11]. Additionally, numerous studies have demonstrated that TA possesses several benefits, such as antimicrobial, antifungal, anticancer properties, and its potential to improve diabetes conditions [12]. In a comparative study, TA exhibited antioxidant activity similar to other antioxidants like butylated hydroxyanisole (BHA), butylated hydroxytoluene (BHT), tocopherol and trolox. [13]. Additionally, TA has been shown to act as a natural iron chelator, a property employed in various applications, such as drug delivery to sustain iron supply and kill cancer cells [14]. Considering the growing body of research highlighting the involvement of ferroptosis in various diseases and the potential benefits of TA as an antioxidant and iron chelator [15], utilizing TA as a ferroptosis inhibitor holds great promise.

In this study, we employed human proximal tubule kidney cells exposed to iron overload and GPX4 inhibition, as well as Wistar rats subjected to iron overload, to investigate the potential antiferroptosis effects of TA. In the in vitro model, even a low dose of TA successfully prevents the deterioration resulting from iron overload and GPX4 inhibition, whereas deferoxamine (DFO), an iron chelator, requires a much higher dose to achieve similar results. Moreover, our in vivo model also yields consistent findings, comparable to the in vitro model, where TA reduces lipid peroxidation induced by ferrous sulfate in the kidney and liver while maintaining kidney and liver parameters at normal levels.

Materials and Methods

Materials

Human Kidney 2 (HK-2) proximal tubular cell was purchased from ATCC (Manassas, VA, USA). Dulbecco's Modified Eagle's Medium (DMEM), phosphate buffered saline (PBS), and 100X penicillin–streptomycin (10,000 U/mL) were purchased from Life Technologies Corporation (Grand Island, NY, USA). Fetal bovine serum (FBS) was purchased from Hyclone (Logan, UT, USA). BioTrace™ nitrocellulose transfer membrane was purchased from Pall (Port Washington, NY, USA). Iron Salophene (FeSP) (28,788), RSL3 (19,288), ML385 (21,114), and TBRAS assay kit (10,009,055) were purchased from Cayman (Ann Arbor, MI, USA). CCK-8 cell counting kit was purchased from Vazyme (Nanjing, China). BODIPY™ 581/591 C11 was purchased from Invitrogen (Waltham, MA, USA). Antibodies against COX2 (#12,282), and TfR1 (#13,113), were purchased from Cell Signaling Technology (Danvers, MA, USA). Antibody against HO-1 (A19062), Nrf2 (A1244), and pNrf2 (AP1133) were purchased from Abclonal Technology (Woburn, MA, USA). Antibodies against GAPDH (sc-32233), mouse and rabbit secondary antibodies were purchased from Santa Cruz Biotechnology (Dallas, TX, USA). Immobilon Western Chemiluminescent HRP Substrate was purchased from Millipore (Burlington, MA, USA). Tannic acid (W304204) and potassium hexacyanoferrate (II) trihydrate (P3289) were purchased from Sigma Aldrich (St. Louis, MO, USA). GenMute™ transfection reagent (SL100568) was purchased from SignaGen® Laboratories (Frederick, MD, USA). SiNrf2 (NFE2L2, 4780) was purchased from Dharmacon, Inc. (Lafayette, CO, USA). Iron Assay Kit (MAK025) was purchased from Sigma Aldrich (St. Louis, MO, USA). FerroOrange was purchased from Dojindo (Kumamoto, JP).

Animal Experiment

Animal experiments were carried out in strict accordance with the National Institutes of Health Guide for Care and Use of Laboratory Animals and with the approval of the Institutional Animal Care and Use Committee (IACUC approval no. 112–10) of Hualien Tzu Chi Hospital. Furthermore, all procedures conducted in the animal study were in accordance with the ARRIVE guidelines.

The sample size for the animals in this study was determined using the resource equation method [16]. The health status of the animals was not evaluated. Upon acquiring the animals, they were provided with a one-week period to acclimatize to the room and cage conditions. Eight-week-old male Wistar rats weighing 180–220 g were utilized for this investigation. All rats were housed in a controlled environment (temperature: 23 ± 1 °C; humidity: 55–60%) under a 12/12-h light/dark cycle, with unrestricted access to food and water.

Tannic acid (TA) was intragastrically administered to three groups of rats at daily doses of 7.5 mg/kg, 15 mg/kg, and 30 mg/kg daily over an 8-day period, with each group receiving a volume of 5 ml/kg. On the 7th and 8th days, Ferrous Sulfate ($FeSO_4$) (300 mg/kg) was administered intragastrically, 30 min after TA administration to induce iron overload [17]. Control group only received water (5 ml/kg) as a vehicle for TA. Subsequently, 24 h later, blood, liver, and kidney samples were collected from the rats under deep isoflurane anesthesia.

Culture of HK-2 cells

HK-2 cells were maintained in DMEM supplemented with 10% FBS and 1X penicillin–streptomycin at 37 °C in a humidified 5% CO2 incubator. Once the cells reached around 90–100% confluence, they were seeded in 6-well or 12-well culture plates for experiments. Before TA, FeSP, RSL3, and ML385 treatments, the growth media

was replaced with DMEM/F-12 without serum to make the cells quiescent for overnight.

Viability assay

HK-2 cells were cultured in 12-well plates, after they reached 80–90% confluence, the growth media was replaced with DMEM without serum and the cells were incubated at 37 °C for overnight before further treatment. After treatment, the viability of the cells was measured by using CCK-8 assay kit. Briefly, CCK-8 solution was mixed with the growth media (20µL/mL) and 500 µL was added to each well and incubated for 2 h at 37 °C. The absorbance at 460 nm was measured with Epoch™ BioTek Instruments microplate spectrophotometer.

Lipid ROS Detection

The BODIPY™ 581/591 C11 probe was used to detect lipid ROS generation in HK-2 cells. The BODIPY™ 581/591 C11 was diluted in DMSO to make 1.5 mM stock solution. After treatment, the media was removed, and replaced with working solution of BODIPY™ 581/591 C11 diluted in growth media for 1.25 µM incubated for 30 min in a humidified 37 °C incubator. After incubation, the cells were harvested and subjected to flow cytometry analysis.

Western Blot Analysis

The protocol used was similar to previous studies [18, 19]. Following treatment, the cells were harvested. The media was removed and the cells were washed with PBS. The mixture of 2X Laemmli buffer and 2X RIPA buffer in 1:1 ratio was added to collect the cells. The total protein was measured using Bradford assay kit. Around 20–30 µg of total protein were separated in 10% SDS-PAGE gel for 100 min and 90 V conditions, and then transferred to a nitrocellulose membrane. The membrane was cut according to the desired protein size, and then incubated in primary antibody (1:1000) diluted in 5% BSA at 4 °C for overnight. The following day, the primary antibody solution was removed, and the membrane was washed thrice for 5 min each with tris buffered saline containing 1% Tween 20. Thereafter, the membrane was incubated with appropriate secondary antibody (1:5000) diluted in 5% BSA at RT for 1 h. Finally, chemiluminescent substrate was used to visualize the proteins. The signal was captured by using UVP ChemStudio Plus touch (Analytik Jena; Jena, Germany). The images were quantified using ImageJ (NIH).

Immunofluorescence Staining

The protocol for immunofluorescence staining has been described in the previous study [20]. Briefly, the cells were fixed with 4% paraformaldehyde after treatment for 5 min, followed by washing with PBS thrice for few seconds. Next, 1% BSA was added to block the unspecific binding of antibodies for 30-min at RT. After blocking, the cells were incubated with primary antibody overnight at 4 °C. The following day, the primary antibody solution was removed, and the cells were washed with PBS thrice. Finally, a secondary antibody was added for one hour at RT. The cells were mounted with DAPI solution and covered with coverslips. The images were taken using fluorescence microscopy (Olympus).

Intracellular Fe^{2+} Detection

FerroOrange was used to detect intracellular Fe^{2+} accumulation assessed by flowcytometry. Briefly, after 16 h treatment the cells were trypsinized, followed by washing with PBS once. Next, the cells were incubated in 37 °C incubator for 30 min with 1 µmol/l FerroOrange working solution. After incubation, the cells were subjected to flow cytometry analysis.

Serum Parameters

The serum blood parameters were assessed by automated analyzer for clinical chemistry (SPOTCHEM EZ SP-4430). Briefly, blood was collected during animal sacrifice. The blood was centrifuged, serum was isolated and then kept at – 80 °C for later analysis of BUN and ALT.

Thiobarbituric Acid Reactive Substances (TBRAS) Measurement

Liver and kidney tissues were subjected to sonication to disrupt the tissue structure. Subsequently, the protein content was quantified. The TBRAS measurements were performed using an equal amount of protein from each sample, following the instructions provided in the TBRAS kit. In brief, 25 µl of the sample was mixed and vortexed with 25 µl of SDS solution. Then, 1 ml of a color reagent, comprising a mixture of thiobarbituric acid diluted with acetic acid and sodium hydroxide, was added, and the mixture was boiled at 100 °C for 1 h. Afterward, the sample was promptly placed on ice to halt the reaction for 10 min, followed by centrifugation, and the absorbance was read at 530 nm using an ELISA reader.

Tissue Iron Staining

Liver and kidney tissues, which had been fixed in formalin, were sliced to a thickness of 20 µm. Subsequently, the tissues underwent Prussian Blue staining by immersing them in a mixture of equal parts of a 20% aqueous solution of hydrochloric acid and a 10% aqueous solution of potassium ferrocyanide for a duration of 20 min. Following the staining process, the tissues were thoroughly rinsed with distilled water and then dehydrated sequentially with 95% and 100% ethanol. Finally, they were immersed in xylene.

Tissue Iron Measurement

The tissue iron measurement procedure was conducted following the company's protocol. Briefly, approximately 50 mg of wet tissue was homogenized by sonication in 200 µl of iron assay buffer, followed by centrifugation at 16,000 × g for 10 min at 4 °C. Fifty µl of the sample was used for measurement in a 96-well plate. Five µl of iron reducer was added to each sample and incubated at room temperature for 30 min. Subsequently, 100 µl of iron probe was added to each sample and incubated again for 60 min at room temperature before finally being read at 593 nm using ELISA reader.

SiRNA Transfection

After the HK-2 cells reached approximately 50% confluence, the medium was removed and replaced with fresh medium supplemented with 10% FBS. After 1 h, the cells were transfected with a 50 nM Si-Nrf2 complex using GenMute™ transfection reagent for 8 h in a humidified 37 °C incubator. Subsequently, the medium was replaced with serum-free medium for 16 h before treatment with FeSP or TA.

Statistical Analysis

The data were presented as mean ± S.E.M. and were statistically analyzed and graphed using GraphPad Prism version 7.0.0. All data were assumed to follow a normal distribution. One-way ANOVA and post hoc Dunnett multiple comparisons were conducted. A p-value of < 0.05 was regarded as statistically significant.

Results

Effect of Tannic Acid, FeSP, and RSL3 on Cell Viability of HK-2 Cells

To assess the optimal concentration and cytotoxicity in HK-2 cells, we conducted a viability assay. In Fig. 1A, we demonstrated that a 24-h incubation with TA, up to a concentration of 5 µM, does not adversely affect the viability of HK-2 cells. Ferroptosis is closely associated with lipid peroxidation within cells. Therefore, when lipid peroxidation levels rise, it can lead to the damage of cell membranes, indicating the occurrence of ferroptosis. In Figs. 1B and C, we presented that the concentration for inducing ferroptosis

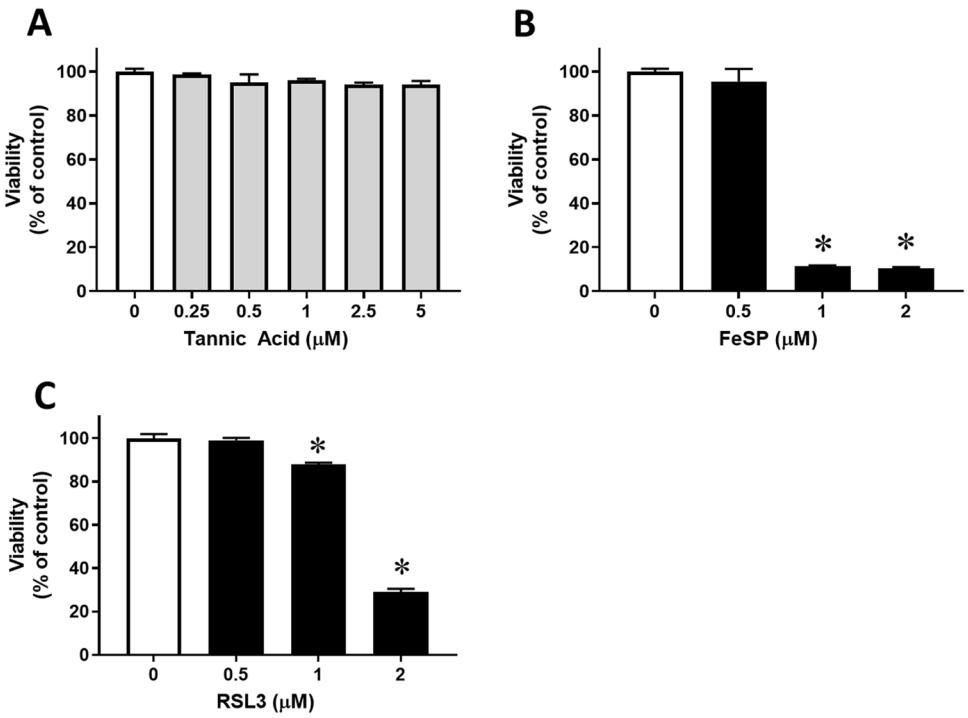

Fig. 1 Effect of various concentrations of tannic acid (TA), FeSP, and RSL3 on viability of HK-2 cells (**A**). Cell viability of HK-2 cells after incubation with TA for 24 h. (**B**) Cell viability of HK-2 cells after incubation with FeSP for 16 h. (**C**) Cell viability of HK-2 cells after incubation with RSL3 for 16 h. N = 3 for each group. *p < 0.05 compared to control, analyzed by one-way ANOVA followed by Dunnett post-test

in HK-2 cells is 1 μM for FeSP and 2 μM for RSL3 during a 16-h incubation. Doubling the dosage did not result in a significant further reduction in cell viability. This suggests that, at this concentration, lipid peroxidation exceeds the threshold that HK-2 cells can withstand.

Tannic Acid Confers Better Protection from Ferroptosis than Deferoxamine

TA is well-known as an iron chelator. In Fig. 2A, as little as 0.25 μM of TA provided complete protection from ferroptosis induced by 1 μM FeSP. In Fig. 2B, we demonstrated that TA prevented ferroptosis induced by 2 μM RSL3 in a dose-dependent manner, with 1 μM of TA offering 100% protection. We compared this to DFO, a commonly used iron chelator, which had been previously tested to prevent ferroptosis [1]. Our results indicate that DFO provides approximately 80% protection from ferroptosis induced by FeSP at 0.25 μM and complete protection at 5 μM (Fig. 2C). However, DFO does not provide any protection when cells are induced by RSL3 (Fig. 2D). Furthermore, we displayed bright field images of the cells to visually illustrate the protective effects of TA and DFO (Fig. 2E, F). In Fig. 2G, we also demonstrated that TA attenuates the elevation of lipid ROS 8 h after FeSP treatment.

Tannic Acid Stabilizes the Expression of Molecular Markers Associated with Ferroptosis

In previous studies, various ferroptosis markers such as TfR1 and COX2 have been identified. However, our findings, as shown in Fig. 3A, indicate that TA has no significant impact on Nrf2, pNrf2, HO-1, or COX2 expression (results not displayed as no discernible expression was observed). Treatment with both FeSP (Fig. 3B) and RSL3 (Fig. 3C) led to a reduction in Nrf2 and pNrf2 levels, accompanied by an increase in COX2 expression. In Fig. 3D, a clear increase in TfR1 levels was observed in cells treated with FeSP for 8 h, alongside a decrease in HO-1 and Nrf2 expression following a 16-h FeSP treatment. Interestingly, the addition of TA resulted in reduced TfR1 expression while increasing both HO-1 and Nrf2 expression, although TA alone did not induce the expression of these proteins. TA has been known to have chelating activity towards iron. In Fig. 3E, we showed that FeSP treatment increases intracellular Fe^{2+}, one of the markers of ferroptosis. As expected, TA treatment concentration-dependently reduces the accumulation of intracellular Fe^{2+}.

The Protection of Tannic Acid is Independent of Nrf2

Nrf2 functions as a central regulator of antioxidant defense. Previous studies have highlighted Nrf2's critical role in mitigating ferroptosis and lipid peroxidation. In our earlier research, we utilized ML385, the only pharmacological inhibitor designed specifically for Nrf2 inhibition. In that study, we demonstrated significant toxicity when combining ML385 with RSL3 [8]. In Fig. 4, we employed non-toxic concentrations of both FeSP and ML385. Consistent with our previous findings, the inhibition of Nrf2 by ML385 resulted in heightened toxicity, even when challenged with non-toxic doses of FeSP (Fig. 4A). Nonetheless, TA continued to protect cells from ferroptosis, indicating its Nrf2-independent efficacy. In addition to pharmacological inhibition, we also employed Si-Nrf2 transfection to knock down Nrf2. Similarly, despite the reduced expression and activity of Nrf2, leading to the absence of HO-1 expression, TA still exhibits its protective effect (Fig. 4B). We also showcased TA's Nrf2-independent protective effect by examining the expression of antioxidant proteins such as Nrf2, pNrf2 and HO-1 (Fig. 4C and D). To strengthen this observation, we assessed the definitive marker of ferroptosis, lipid ROS, and observed that Nrf2 inhibition led to a ~ tenfold increase in lipid ROS levels in the presence of FeSP. However, TA pretreatment prevented this effect, maintaining lipid ROS levels comparable to the control group (Fig. 4E).

Tannic Acid Prevents Liver and Kidney Dysfunction in Male Rats Fed by $FeSO_4$

To assess TA's protective effects in vivo, we administered TA to male albino rats for 8 days. On the 7th and 8th day, we subjected the rats to an intragastric dose of $FeSO_4$ (300 mg/kg). On the 9th day, the rats were sacrificed, and blood, liver, and kidney samples were collected. In Fig. 5A, we observed that BUN levels, an indicator of kidney function, were elevated in rats fed with $FeSO_4$. Figure 5B illustrates that ALT levels, an indicator of liver function, were also elevated in the $FeSO_4$-fed rats. However, all tested doses of TA significantly lowered BUN and ALT levels, indicating TA's protective effects. We further corroborated these findings with TBRAS assays, which measure lipid peroxidation. $FeSO_4$-treated rats displayed higher TBRAS levels in both the kidney (Fig. 5C) and liver (Fig. 5D), which TA effectively prevented. Additionally, we examined the expression of several proteins, including Nrf2, pNrf2, and HO-1 (Fig. 5E and 5F). Generally, our observations in rats mirrored those in HK-2 cells. In both kidney and liver, $FeSO_4$ treatment induced HO-1 expression, which was not observed in the TA-treated group. This suggests that since HO-1 expression serves as a protective response to external stress, such as $FeSO_4$, it increased in the kidney and liver. However, due to TA's ability to trap iron and radicals, lipid ROS levels did not increase, resulting in the absence of HO-1 expression in this group.

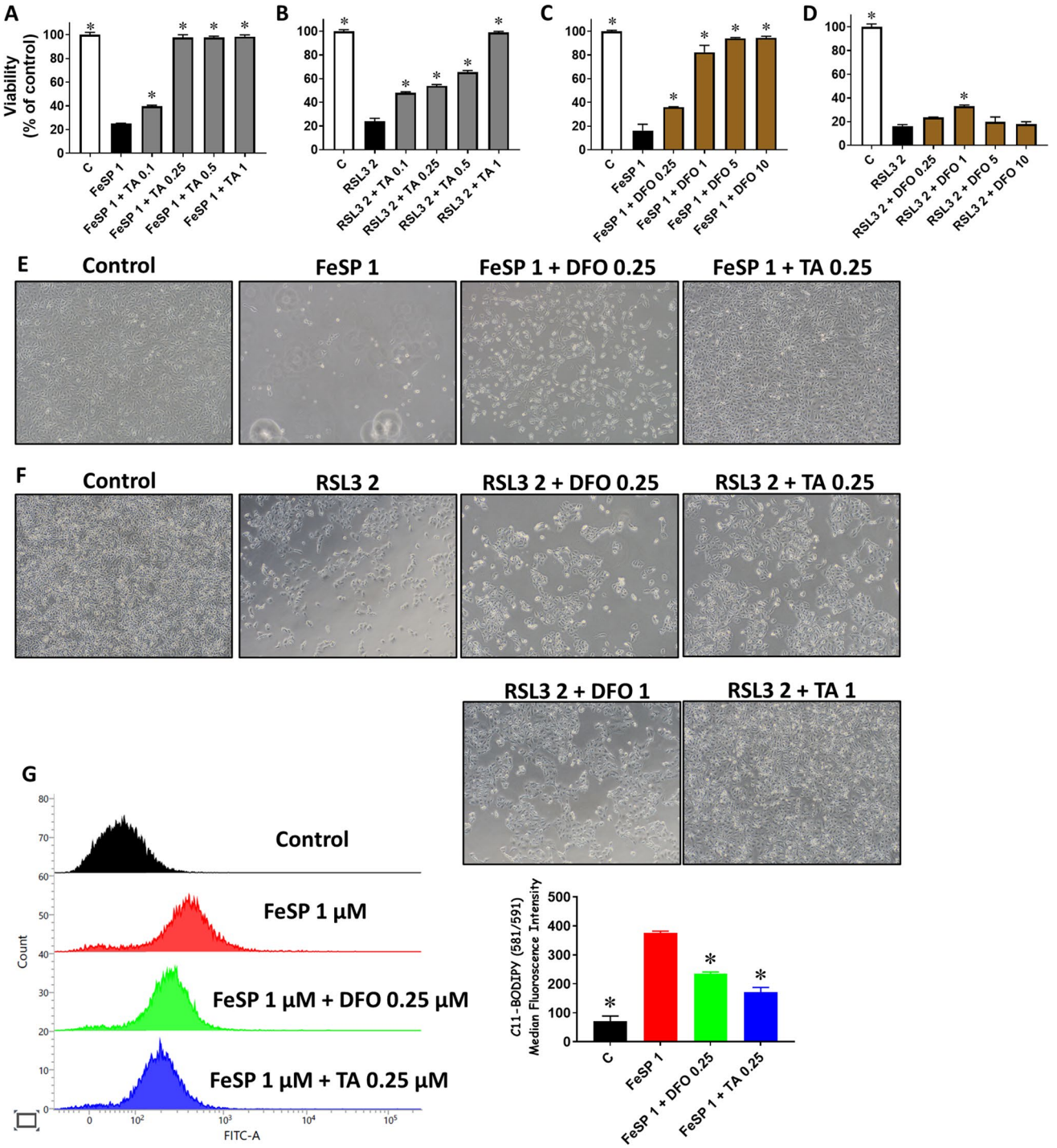

Fig. 2 Comparison between the protective effects of tannic acid (TA) and a renowned iron chelator, deferoxamine (DFO). (**A**) Cell viability of HK-2 cells after incubation with FeSP or (**B**) RSL3 for 16 h with or without TA pretreatment for 1 h. (**C**) Cell viability of HK-2 cells after incubation with FeSP or (**D**) RSL3 for 16 h with or without DFO pretreatment for 1 h. (**E**) Brightfield image with 10X magnification of HK-2 cells after incubation with FeSP or (**F**) RSL3 for 16 h with or without TA or DFO pretreatment for 1 h. (**G**) Lipid ROS level assessed by flowcytometry in HK-2 cells after incubation with FeSP for 8 h with or without TA or DFO pretreatment for 1 h. N = 3 for each group. *$p < 0.05$ compared to FeSP or RSL3, analyzed by one-way ANOVA followed by Dunnett post-test

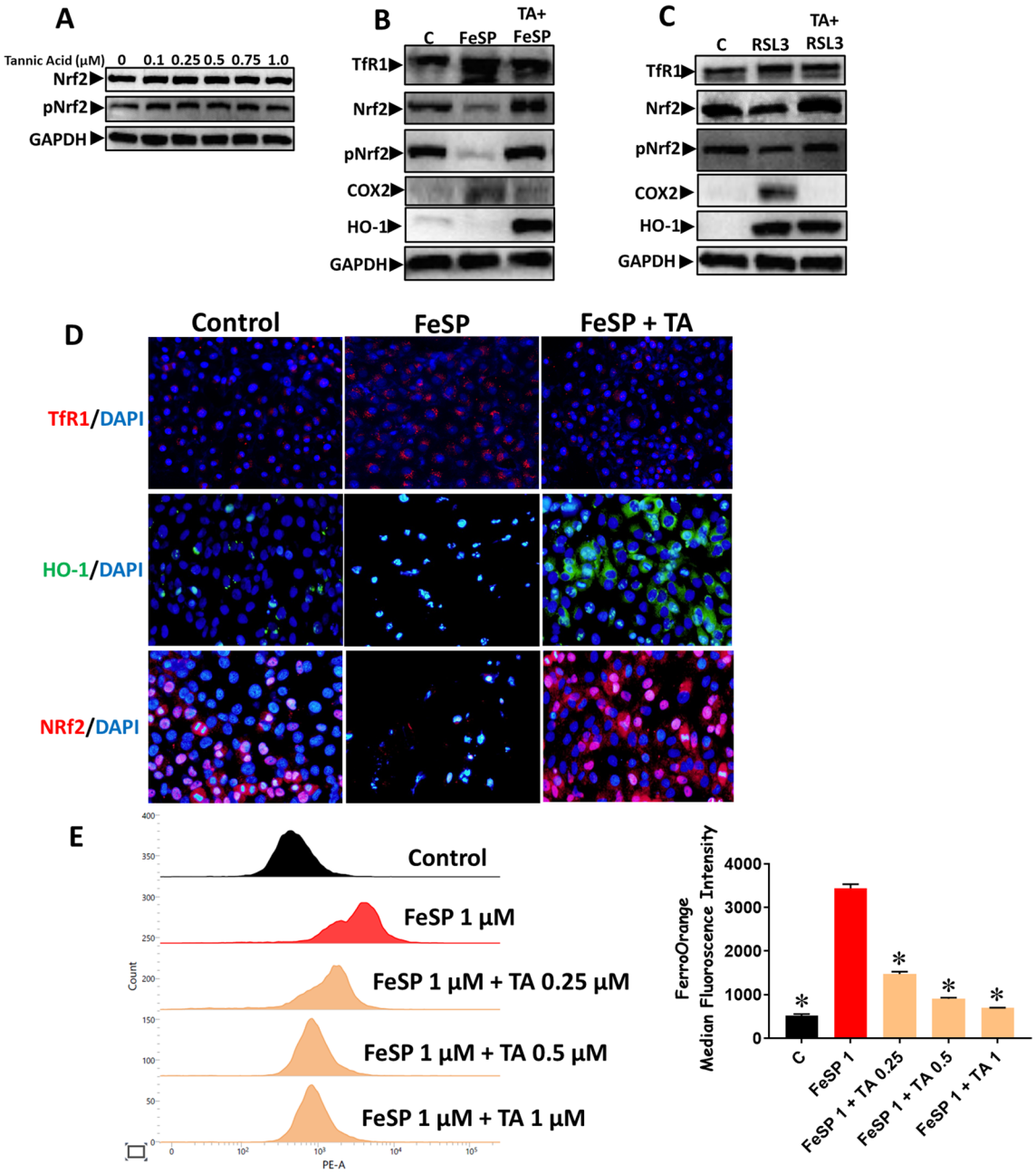

Fig. 3 Evaluation of various ferroptosis markers in HK-2 cells exposed to FeSP or RSL3 and subjected to tannic acid treatment. (**A**) TA shows no apparent effect on Nrf2 and pNrf2 for 24 h incubation (**B**) Western blot analysis of ferroptosis marker in HK-2 cells treated with FeSP (1 μM) or (**C**) RSL3 (2 μM) for 16 h with or without 1 h TA (0.25 μM in FeSP and 1 μM in RSL3) pretreatment. (**D**) Immunofluorescence image with 10X magnification of TfR1 after 8 h incubation with FeSP (1 μM), and HO-1 and Nrf2 after 16 h incubation with FeSP (1 μM) with or without 1 h pretreatment with TA (0.25 μM). (**E**) Intracellular Fe^{2+} detected by FerroOrange after 16 h incubation with FeSP (1 μM) with or without 1 h pretreatment with TA analyzed by flowcytometry. *$p < 0.05$ compared to FeSP, analyzed by one-way ANOVA followed by Dunnett post-test

Tannic Acid Inhibits iron Accumulation in Ahe Liver and Kidney Triggered by $FeSO_4$

Due to its large molecular size and poor bioavailability, TA is known to have limited absorption. As anticipated, the administration of a high dose of $FeSO_4$ resulted in substantial iron accumulation in both the liver and kidney as evidenced by the Prussian Blue staining (Fig. 6A), and tissue iron measurement (Fig. 6B). Both TA and $FeSO_4$ were administered intragastrically. In this context, we hypothesized that TA would form complexes with iron, reducing its absorption and tissue accumulation. As

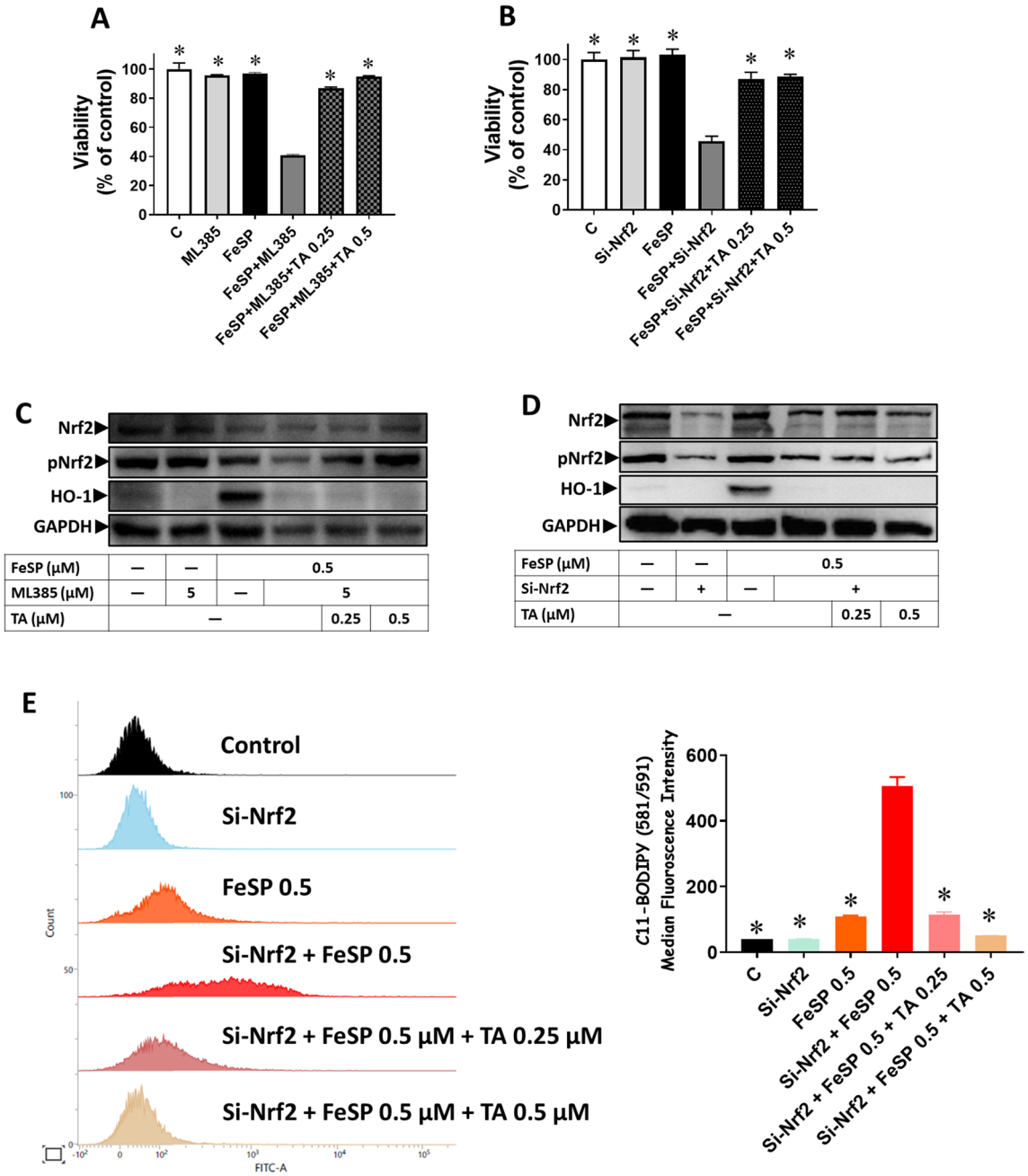

Fig. 4 The protective effect of TA is independent of Nrf2. (**A**) Viability of HK-2 cells subjected to ML385 (5 μM) pretreatment for 1 h, or (**B**) transfected with Si-Nrf2 for 8 h, followed by TA (0.25 μM or 0.5 μM) for 1 h, and FeSP (0.5 μM) for 16 h. (**C**) Western blot analysis of antioxidant protein in HK-2 cells subjected to ML385 (5 μM) pretreatment for 1 h, or (**D**) transfected with Si-Nrf2 for 8 h, followed by TA (0.25 μM or 0.5 μM) for 1 h, and FeSP (0.5 μM) for 16 h. (**E**) Lipid ROS level assessed by flowcytometry in HK-2 cells after transfection with Si-Nrf2 for 8 h, followed by TA (0.25 μM or 0.5 μM) for 1 h, and FeSP (0.5 μM) for 8 h. N = 3 for each group. *p < 0.05 compared to FeSP + ML385 or FeSP + Si-Nrf2, analyzed by one-way ANOVA followed by Dunnett post-test

expected, treatment with TA (7.5 mg/kg) effectively prevented iron accumulation, with results comparable to the control group. This suggests that, in addition to its antioxidant properties, TA's significant effect may primarily stem from its iron-chelating activity.

Discussion

Iron accumulation is a core factor that increases lipid peroxidation, leading to ferroptosis [3]. Elevated levels of

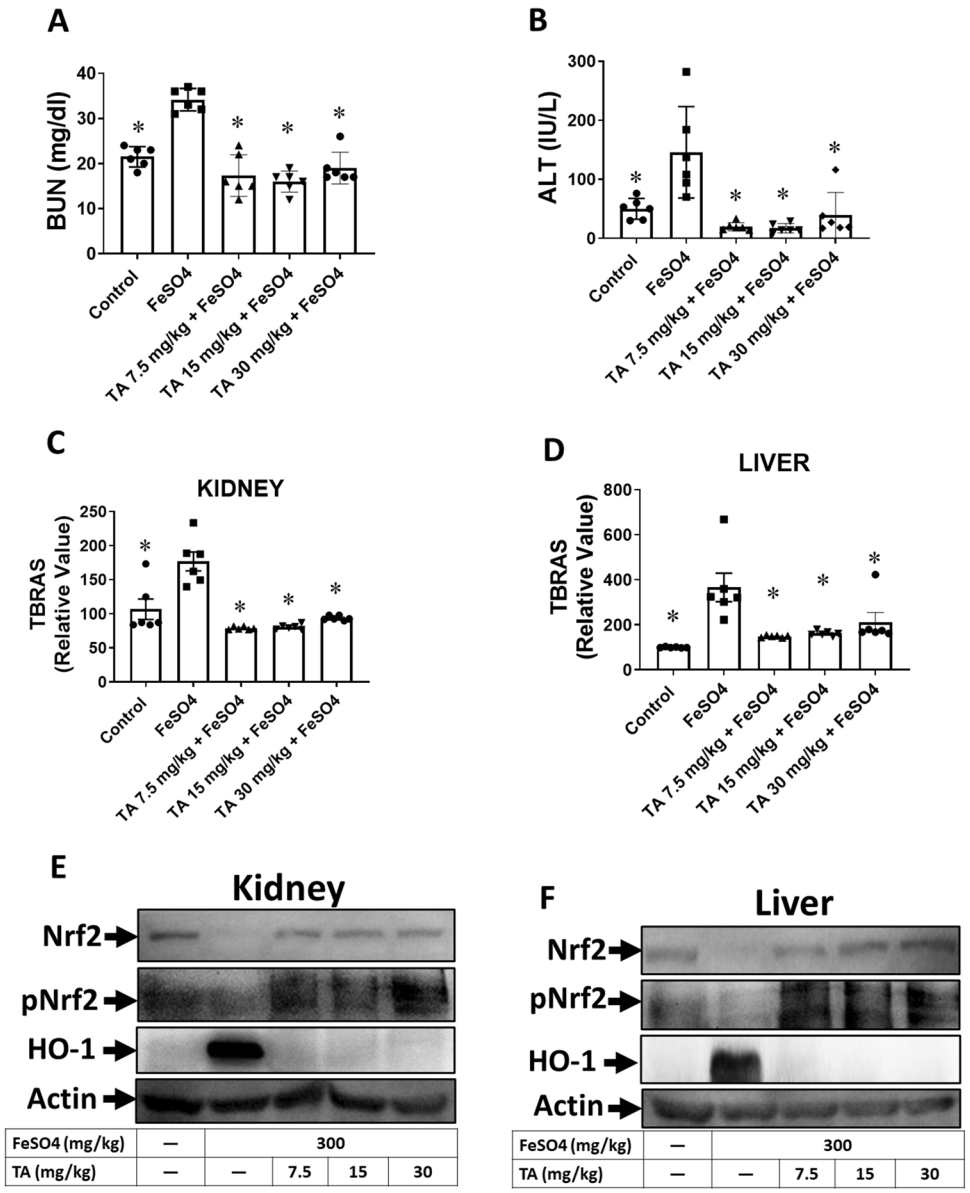

Fig. 5 Eight days intragastric tannic acid administration protects the kidney and liver from intragastric $FeSO_4$ (300 mg/kg) (**A**) BUN and (**B**) ALT level in serum of rats. (**C**) TBRAS level in homogenize kidney tissue and (**D**) liver tissue. (**F**) Western blot analysis of antioxidant protein in kidney and (**E**) liver of rats. N = 6 for each group. Values are presented as mean ± SEM. *p < 0.05 compared to the $FeSO_4$, analyzed by one-way ANOVA followed by Dunnett post-test

lipid peroxidation, followed by membrane damage, are clear indications of ferroptosis. Numerous studies and reviews have established that ferroptosis plays a crucial role in various diseases and is a target for drug development [21]. Several potent ferroptosis inhibitors, such as Ferrostatin-1, Liproxstatin-1, and UAMC-3203, have been identified to date. However, the concept of iron toxicity in ferroptosis and the development of drugs to address this aspect have received limited attention, with only a few studies exploring this area. A recent study has shown that plasma iron levels and lipid peroxidation of critically ill patients exhibit a strong correlation with the severity of multiorgan dysfunction. That study even went a step further and used an iron toxicity model in mice to explore potential of UAMC-3203 as antiferroptosis drugs [6]. Iron toxicity in humans is a well-documented concern. A report from 2020 documented a total of 3625 instances of unintended ingestion of iron or iron salts [22], indicating an increasing trend compared to 2014, when 3211 cases were reported [23]. The clinical spectrum of iron toxicity is extensive, spanning a range of manifestations including gastrointestinal discomfort, emesis, diarrhea, impaired hepatic function, renal insufficiency, and, in exceptional cases, mortality.

Previous studies have shown that TA can inhibit erastin-induced ferroptosis in stem cell [24]. In this study, we present, for the first time, the robust antiferroptotic properties of tannic acid (TA) both in vitro and in vivo, using iron and RSL3 as inducers of ferroptosis. For the in vitro model, we used kidney cells, as a previous study in mice showed that

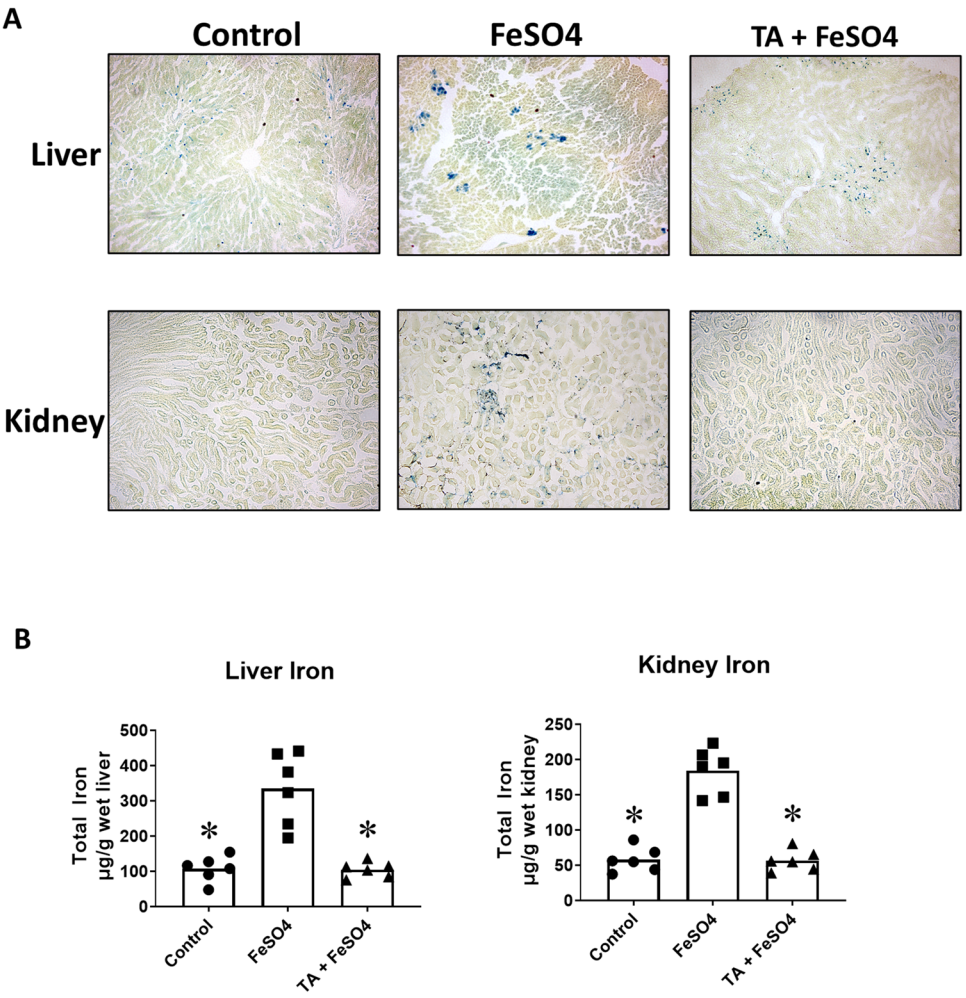

Fig. 6 Tannic acid prevents elevated iron deposition induced by $FeSO_4$ (**A**) Brightfield image with 10X magnification of Prussian blue staining in liver and kidney tissue of rats challenged by $FeSO_4$ (300 mg/kg) with or without 7.5 mg/kg TA treatment. (**B**) Total iron level in wet tissue of liver (left panel) and kidney (right panel) challenged by $FeSO_4$ (300 mg/kg) with or without 7.5 mg/kg TA treatment. N = 6 for each group. *$p < 0.05$ compared to the $FeSO_4$, analyzed by one-way ANOVA followed by Dunnett post-test

the kidney is the most affected organ by iron toxicity using ferrous sulfate ($FeSO_4$) [6]. We employed two ferroptosis inducers in the cell model: one is iron-salophene (FeSP), which mimics iron accumulation leading to ferroptosis, and the second is RAS-selective lethal 3 (RSL3), a glutathione peroxidase 4 inhibitor, which will eventually lead to lipid peroxidation accumulation and ferroptosis. TA demonstrated particular efficacy in mitigating ferroptosis triggered by FeSP or RSL3 in HK-2 cells in a low concentration 1 µM or less. TA is widely recognized for its ability to form complexes with iron, a property that has found applications in various biomedical fields, including drug delivery and cancer research [25]. Studies have demonstrated that TA forms a 1:1 complex with Fe(III) and a 3:1 complex with Fe(II) [26]. Physiologically, the majority of iron is internalized through its binding with transferrin, facilitating its entry into cells through endocytosis. Our findings indicate that FeSP treatment leads to an increase in transferrin receptor protein 1 (TfR1). Consequently, we propose that the elevated levels of TfR1 contribute to an augmentation in cellular iron uptake, potentially facilitating the entry of FeSP into the cells. By using FerroOrange as Fe^{2+} probe, we found that FeSP treatment increases intracellular Fe^{2+}, whereas TA treatment concentration-dependently decreases intracellular Fe^{2+}, confirming its ability to trap iron. However, our finding of increased TfR1 expression in kidney cells appears noncanonical, as iron overload typically leads to a reduction in TfR1 expression as part of the normal cellular mechanism to regulate intracellular iron levels [27]. Additionally, we acknowledge the limitation that this study did not assess TfR1 expression in the tissues of the rats, making it challenging to draw definitive conclusions about TfR1 in iron-induced ferroptosis and toxicity. Further research is needed to explore the role of different iron complexes and other sources of iron in modulating TfR1 and other proteins involved in iron trafficking to address this limitation and enhance our understanding.

TA has been shown to possess strong antioxidant and radical scavenging activity [13]. When exposed to FeSP, TA demonstrated effective cell protection at a low concentration of 0.25 µM. In contrast, the iron chelator DFO exhibited similar efficacy but required a higher dose of > 1 µM for

similar protection. When RSL3 was used, TA showed potent protection at a concentration of 1 μM, whereas DFO failed to provide any protection, even at a concentration of 10 μM. One possible explanation for the lack of protective effects observed with DFO in the presence of RSL3, a ferroptosis inducer, could stem from the distinct mechanism by which ferroptosis is induced. RSL3 triggers ferroptosis by reducing or eliminating GPX4 levels. GPX4 plays a crucial role in catalyzing the reduction of lipid ROS into lipid alcohols, directly counteracting lipid ROS. Given that DFO acts as an iron chelator, its inability to confer protection in the context of RSL3-induced ferroptosis can be reasonably understood. These results indirectly imply that TA's antiferroptotic activity arises from its iron-chelating capabilities and its radical-trapping ability, attributed to its polyphenolic nature. Our investigation in vivo revealed that the intragastric administration of as little as 7.5 mg/kg of TA to rats effectively reduces the elevated levels of malondialdehyde (MDA) and iron accumulation induced by intragastric administration of $FeSO_4$ in the liver and kidney of rats, which serve as a model for iron overload. Notably, the results of kidney and liver parameters, including blood urea nitrogen (BUN) and alanine aminotransferase (ALT), provided additional support for our hypothesis that TA confers a strong protective effect against iron-induced liver and kidney dysfunction. However, comparing TA's activity with other ferroptosis inhibitors that act as radical traps, such as Ferrostatin-1, is essential. We acknowledge this as a limitation of our study and recommend that future research include comparisons with other ferroptosis inhibitors to provide a more comprehensive understanding.

Nrf2 is a transcription factor responsible for regulating numerous antioxidant genes and plays a role in protecting cells from ferroptosis [28]. Moreover, it also plays role in controlling iron homeostasis [29]. In a previous study, we discovered that the use of an Nrf2 inhibitor, ML385, resulted in increased toxicity in cells treated with RSL3 [8]. In our current study, we observed a significant decrease in Nrf2 expression when cells were treated with RSL3 and FeSP, and this decrease was prevented by TA treatment. Interestingly, TA treatment alone did not increase Nrf2 expression. Our results also suggest that TA's protective effect operates independently of Nrf2 since inhibiting Nrf2 with ML385 or Nrf2 knockdown with Si-Nrf2 did not diminish the protection provided by TA against ferroptosis induced by FeSP.

The Nrf2 and heme-oxygenase 1 (HO-1) axis is known to be involved in RSL3-induced ferroptosis. Our results in both TA with FeSP or TA with RSL3 shows increase in HO-1 expression. However, when TA was administered alone, there was no noticeable increase in HO-1 expression (results are not shown). Prior research has already indicated that HO-1 plays a crucial role in reducing ferroptosis. This was demonstrated when kidney cells lacking HO-1 displayed increased sensitivity to ferroptosis inducers [9]. In our research, we observed a significant difference in the expression of HO-1 when comparing the use of a lethal concentration of FeSP (Fig. 3B) and a non-lethal concentration (Fig. 4B). Specifically, we noted that HO-1 did not express at all when the high dose of FeSP was administered. We interpret this finding as follows: when a high dose of FeSP is used, it leads to a substantial increase in lipid ROS levels and a significant suppression of Nrf2 expression and activity. These factors collectively contribute to the absence of HO-1 expression at higher FeSP doses. In contrast, when a non-lethal concentration of FeSP is employed, it appears to elevate lipid ROS levels to a moderate extent. We also observed that when RSL3 was used, HO-1 was upregulated. We suggest there was a speculative increase in lipid ROS when HO-1 is upregulated, which triggers the cell antioxidant system. In this case, it is orchestrated by Nrf2, leading to the upregulation of HO-1. However, it is important to note that a more comprehensive investigation is required to delve deeper into this phenomenon and understand the underlying mechanisms at play. We also noted an increase in COX2 levels both with FeSP and RSL3. While COX2 is traditionally recognized as a key player in inflammation, recent research has suggested its potential as a specific marker for ferroptosis. However, attempts to inhibit COX2 during ferroptosis do not result in a reduction in ferroptosis levels, confirming its role as a downstream marker rather than a causative factor in ferroptosis [30]. In our experiments, we observed an increase in COX2 expression when cells were treated with either FeSP or RSL3, and this elevated expression was almost completely diminished when treated with TA.

A limitation of our study is that, while the iron dose used in this research is considered high and potentially toxic to humans, no behavioral changes or pain symptoms in the rats were observed at least 24 h after iron ingestion. Nonetheless, our study demonstrated that iron in the form of $FeSO_4$ at a dose of 300 mg/kg resulted in increased lipid ROS, elevated levels of BUN and ALT, as well as iron deposition in the liver and kidney of the rats. This parallels the effects observed in humans following high dose of iron ingestion.

Due to its antioxidant capacity, coupled with iron-chelating properties, TA may offer potential benefits in cases of accidental iron ingestion. However, its route of administration is limited to oral consumption, as other methods such as intravenous or subcutaneous administration can be toxic [31]. TA is poorly absorbed in its unmetabolized form through gastrointestinal (GI) system hence the beneficial effect of TA we showed in this study is likely due to its iron chelating activity in the GI track which inhibit the absorbtion of iron into circulation. Nonetheless, TA can be metabolized into gallic acid, pyrogallol, or resorcinol and absorbed into circulation which although lost iron chelating activity however still posseses antioxidant activity [32]. The

iron-chelating ability of TA arises from its multiple phenolic hydroxyl groups. However, when the ester bonds in TA are hydrolyzed, free gallic acid is released, leading to a loss of this chelating capacity. Despite this, gallic acid, which still contains phenolic hydroxyl groups, can continue to function as an antioxidant through H + transfer [33]. According to the European Food Safety Authority, TA is considered safe for consumption as a food additive at levels up to 15 mg/kg. Previous studies have investigated TA's specific chelation properties, revealing its ability to selectively affect serum iron levels without interfering with essential minerals like zinc, copper, and manganese [34]. This characteristic further suggests that TA might be beneficial for conditions associated specifically with elevated iron levels. For instance, TA could have potential utility in individuals with hemochromatosis, a condition characterized by the excessive accumulation of iron in tissues and organs. Since the body does not produce iron, supplementing with TA alongside food (source of iron) could potentially provide therapeutic benefits for people with hemochromatosis. However, further research is needed to fully investigate and confirm these potential applications.

Authors' Contributions IPT: Conceptualization, Methodology, Investigation, Formal analysis, Validation, Writing- Original Draft, Funding acquisition. ST: Supervision, Project administration, Funding acquisition. SH: Supervision, Project administration, Funding acquisition. LYY: Supervision, Project administration. CYH: Supervision, Project administration, Funding acquisition. JHS: Conceptualization, Methodology, Data curation, Formal analysis, Investigation, Writing- Original Draft, Writing- Reviewing & Editing.

Funding This study was supported by Universitas Muhammadiyah Yogyakarta, Indonesia (Grant number: 56/R-LRI/XII/2022), Buddhist Tzu Chi General Hospital (Grant number: IMAR-111–01-08) and by the Ministry of Science and Technology, Taiwan (Grant number: MOST 110–2314-B-303–006).

Data Availability No datasets were generated or analysed during the current study.

Declarations

Competing Interests The authors declare no competing interests.

References

1. Dixon SJ et al (2012) Ferroptosis: an iron-dependent form of nonapoptotic cell death. Cell 149(5):1060–1072
2. Tan S, Schubert D, Maher P (2001) Oxytosis: A novel form of programmed cell death. Curr Top Med Chem 1(6):497–506
3. Dixon SJ, Pratt DA (2023) Ferroptosis: A flexible constellation of related biochemical mechanisms. Mol Cell 83(7):1030–1042
4. Jiang X, Stockwell BR, Conrad M (2021) Ferroptosis: mechanisms, biology and role in disease. Nat Rev Mol Cell Biol 22(4):266–282
5. Han C et al (2020) Ferroptosis and Its Potential Role in Human Diseases. Front Pharmacol 11:239
6. Van Coillie S et al (2022) Targeting ferroptosis protects against experimental (multi)organ dysfunction and death. Nat Commun 13(1):1046
7. Friedmann Angeli JP et al (2014) Inactivation of the ferroptosis regulator Gpx4 triggers acute renal failure in mice. Nat Cell Biol 16(12):1180–1191
8. Taufani IP et al (2023) Mitochondrial ROS induced by ML385, an Nrf2 inhibitor aggravates the ferroptosis induced by RSL3 in human lung epithelial BEAS-2B cells. Hum Exp Toxicol 42:9603271221149664
9. Adedoyin O et al (2018) Heme oxygenase-1 mitigates ferroptosis in renal proximal tubule cells. Am J Physiol Renal Physiol 314(5):F702–F714
10. Seibt TM, Proneth B, Conrad M (2019) Role of GPX4 in ferroptosis and its pharmacological implication. Free Radic Biol Med 133:144–152
11. Baldwin A, Booth BW (2022) Biomedical applications of tannic acid. J Biomater Appl 36(8):1503–1523
12. Liu X et al (2005) Tannic acid stimulates glucose transport and inhibits adipocyte differentiation in 3T3-L1 cells. J Nutr 135(2):165–171
13. Gülçin İ et al (2010) Radical scavenging and antioxidant activity of tannic acid. Arab J Chem 3(1):43–53
14. Liu T et al (2018) Ferrous-Supply-Regeneration Nanoengineering for Cancer-Cell-Specific Ferroptosis in Combination with Imaging-Guided Photodynamic Therapy. ACS Nano 12(12):12181–12192
15. Phiwchai I et al (2018) Tannic acid (TA): A molecular tool for chelating and imaging labile iron. Eur J Pharm Sci 114:64–73
16. Arifin WN, Zahiruddin WM (2017) Sample Size Calculation in Animal Studies Using Resource Equation Approach. Malays J Med Sci 24(5):101–105
17. Refaat B et al (2018) Acute and Chronic Iron Overloading Differentially Modulates the Expression of Cellular Iron-homeostatic Molecules in Normal Rat Kidney. J Histochem Cytochem 66(11):825–839
18. Lin YM et al (2022) ZAKbeta Alleviates Oxidized Low-density Lipoprotein (ox-LDL)-Induced Apoptosis and B-type Natriuretic Peptide (BNP) Upregulation in Cardiomyoblast. Cell Biochem Biophys 80(3):547–554
19. Loh CH et al (2023) PKC-delta-dependent mitochondrial ROS attenuation is involved as 9-OAHSA combats lipoapotosis in rat hepatocytes induced by palmitic acid and in Syrian hamsters induced by high-fat high-cholesterol high-fructose diet. Toxicol Appl Pharmacol 470:116557
20. Situmorang JH et al (2023) 9-POHSA prevents NF-kB activation and ameliorates LPS-induced inflammation in rat hepatocytes. Lipids 58(5):241–249
21. Yan HF et al (2021) Ferroptosis: mechanisms and links with diseases. Signal Transduct Target Ther 6(1):49
22. Gummin DD et al (2021) 2020 Annual Report of the American Association of Poison Control Centers' National Poison Data System (NPDS): 38th Annual Report. Clin Toxicol (Phila) 59(12):1282–1501
23. Mowry JB et al (2015) 2014 Annual Report of the American Association of Poison Control Centers' National Poison Data System (NPDS): 32nd Annual Report. Clin Toxicol (Phila) 53(10):962–1147
24. Liu Y et al (2021) Tannic Acid as a Natural Ferroptosis Inhibitor: Mechanisms and Beneficial Role of 3'-O-Galloylation. ChemistrySelect 6(7):1562–1569
25. Youness AR et al (2021) Recent Advances in Tannic Acid (Gallotannin) Anticancer Activities and Drug Delivery Systems for Efficacy Improvement; A Comprehensive Review. Molecules 26(5)
26. Fu Z, Chen R (2019) Study of Complexes of Tannic Acid with Fe(III) and Fe(II). J Anal Methods Chem 2019:3894571

27. Camaschella C, Nai A, Silvestri L (2020) Iron metabolism and iron disorders revisited in the hepcidin era. Haematologica 105(2):260–272
28. Dodson M, Castro-Portuguez R, Zhang DD (2019) NRF2 plays a critical role in mitigating lipid peroxidation and ferroptosis. Redox Biol 23:101107
29. Anandhan A et al (2023) NRF2 controls iron homeostasis and ferroptosis through HERC2 and VAMP8. Sci Adv 9(5):eade9585
30. Yang WS et al (2014) Regulation of ferroptotic cancer cell death by GPX4. Cell 156(1–2):317–331
31. Robinson HJ, Graessle OE (1943) TOXICITY OF TANNIC ACID. J Pharmacol Exp Ther 77(1):63
32. Nakamura Y, Tsuji S, Tonogai Y (2003) Method for analysis of tannic acid and its metabolites in biological samples: application to tannic acid metabolism in the rat. J Agric Food Chem 51(1):331–339
33. Li X (2017) 2-Phenyl-4,4,5,5-tetramethylimidazoline-1-oxyl 3-Oxide (PTIO(*)) Radical Scavenging: A New and Simple Antioxidant Assay In Vitro. J Agric Food Chem 65(30):6288–6297
34. Afsana K et al (2004) Reducing effect of ingesting tannic acid on the absorption of iron, but not of zinc, copper and manganese by rats. Biosci Biotechnol Biochem 68(3):584–592

Authors and Affiliations

Indra Putra Taufani[1,2] · Sri Tasminatun[3] · Sabtanti Harimurti[3] · Liang-Yo Yang[4,5] · Chih-Yang Huang[6,7,8,9,10] · Jiro Hasegawa Situmorang[11]

✉ Liang-Yo Yang
yangly@mail.cmu.edu.tw

✉ Chih-Yang Huang
cyhuang@mail.cmu.edu.tw

✉ Jiro Hasegawa Situmorang
jiro.hasegawa.situmorang@brin.go.id;
jiro.hasegawa.s@gmail.com

[1] Graduate Institute of Pharmacy, China Medical University, Taichung, Taiwan

[2] Department of Pharmacist Profession Education, Faculty of Medicine and Health Sciences, Universitas Muhammadiyah Yogyakarta, Yogyakarta, Indonesia

[3] School of Pharmacy, Faculty of Medicine and Health Sciences, Universitas Muhammadiyah Yogyakarta, Yogyakarta, Indonesia

[4] Department of Physiology, School of Medicine, College of Medicine, China Medical University, Taichung, Taiwan

[5] Laboratory for Neural Repair, China Medical University Hospital, Taichung, Taiwan

[6] Cardiovascular and Mitochondrial Related Disease Research Center, Buddhist Tzu Chi General, Hospital, Buddhist Tzu Chi Medical Foundation, Hualien, Taiwan

[7] Graduate Institute of Medical Science, China Medical University, Taichung, Taiwan

[8] Department of Medical Research, China Medical University Hospital, China Medical University, Taichung, Taiwan

[9] Department of Biotechnology, Asia University, Taichung, Taiwan

[10] Center of General Education, Tzu Chi University of Science and Technology, Buddhist Tzu Chi Medical Foundation, Hualien, Taiwan

[11] Center for Biomedical Research, National Research and Innovation Agency (BRIN), Cibinong, Indonesia